Sustainable Energy & Fuels

ROYAL SOCIETY OF CHEMISTRY

PAPER

View Article Online
View Journal | View Issue

Cite this: *Sustainable Energy Fuels*, 2021, **5**, 956

Revealing the contribution of singlet oxygen in the photoelectrochemical oxidation of benzyl alcohol†

Ramón Arcas, Eduardo Peris, Elena Mas-Marzá * and Francisco Fabregat-Santiago *

Photoelectrochemical approaches are finding use in the transformation of organic molecules beyond water oxidation and CO_2 reduction. Among the different reactions that can be performed, the selective oxidation of alcohols to aldehydes is a transformation of great interest, as aldehydes are the starting materials for the preparation of more complex organic molecules with high added value. In order to develop efficient photoelectrochemical methodologies for this reaction, it is crucial to reveal all the different parameters that are involved in such light-driven processes. Herein we analyse in detail the effect of the light wavelength and atmosphere on the photoelectrochemical oxidation of benzyl alcohol to benzaldehyde using $BiVO_4$ electrodes. Our studies demonstrate that an important contribution to the oxidation of alcohol is due to UV light-induced production of singlet oxygen, which is also responsible for the formation of hydrogen peroxide in the reaction media. These findings are key for identifying and evaluating the underlying mechanism involved in this type of photoelectrochemically induced oxidation, in order to avoid misinterpretations of the efficiencies.

Received 4th September 2020
Accepted 27th December 2020

DOI: 10.1039/d0se01322f

rsc.li/sustainable-energy

Introduction

During the last decade, photoelectrocatalysis was mostly focussed in the study of the oxidation of H_2O and the reduction of CO_2,[1–3] while its use in the synthesis of more complex organic molecules with high added value was disregarded.[4] Given the high potentials that can be attained in a photoelectrochemical cell (PEC), it should be considered suitable for the preparation of organic products *via* redox transformations that would be difficult to achieve by chemical means. Just recently, a few examples have been described where photoanodes are used to generate added-value organic species.[5,6] For example, $BiVO_4$ and WO_3 anodes were recently used for the photoelectrochemical oxidation of 5-hydroxymethylfurfural,[7] benzylic alcohols,[8–11] furan,[12] tetralines,[9] cyclohexane,[13,14] glycerol[15] and urea.[16] Also of interest is the synthesis of 5,5′-azotetrazolate-based salts using W, Mo co-doped $BiVO_4$ photoanodes[17] and the amination of arenes assisted by α-Fe_2O_3 electrodes.[18]

The selective oxidation of alcohols to aldehydes is a key transformation in organic synthesis. Traditionally, this reaction involves the use of stoichiometric amounts of inorganic and organic oxidants and harsh reaction conditions. Consequently, efforts have been made in order to perform this transformation in a cleaner and environmentally friendly method using homogeneous or heterogeneous catalysts and oxygen.[19–25] Photoelectrocatalysis constitutes an eco-friendly and smart approach for this transformation. When this reaction is performed in a PEC, the oxidation of the substrate is accompanied by the release of H_2 at the cathode.

In many cases, the photooxidation of alcohols requires that the photocatalyst is irradiated with UV light,[26] but this sometimes causes the product to be formed together with over-oxidized compounds.[27,28] Some studies suggest that the irradiation with UV light may increase the efficiency of the oxidation of benzyl alcohol to benzaldehyde,[29] although the reasons justifying the role of UV light in the process are still unclear. Recently, Mokari and co-workers proposed that, in the photocatalytic oxidation of benzyl alcohol under UV irradiation using heterogeneous catalysts, there is a competition between the photocatalytic process and a so-called 'autooxidation process'. This autooxidation was suggested to be a consequence of the photoactivation of small amounts of benzaldehyde present in the reaction media.[30] Aiming to shed some light on the role of UV irradiation in the photocatalytic oxidation of alcohols, herein we carried out a study considering all plausible mechanistic pathways. In the first set of experiments, we detected a photoelectrode-free oxidation of benzyl alcohol, with concomitant formation of H_2O_2 as a persistent side-product. After performing a series of control experiments, we

Institute of Advanced Materials (INAM), Universitat Jaume I, Av. Vicente Sos Baynat s/n, Castellon E-12006, Spain. E-mail: emas@uji.es; fabresan@uji.es

† Electronic supplementary information (ESI) available: Optical and structural characterization of Zr decorated $BiVO_4$ photoanodes; cyclic voltammetry curves of ferrocene/ferrocenium (Fc/Fc^+) used to calibrate the voltage of the reference electrode; cyclic voltammetry experiment showing the effect of water in photoelectrochemical measurements; detection and quantification of H_2O_2 by ^1H NMR; effect of the atmosphere, light and DABCO, an $^1O_2$ quencher, in anthracene and **1** solutions. See DOI: 10.1039/d0se01322f

concluded that this photoelectrode-free oxidation process is a consequence of the formation of singlet oxygen in the reaction media, which is formed upon irradiating O_2-containing solutions with UV light. In addition, we also found that this photoelectrode-free oxidation pathway has an important share in the total efficiency of the system.

Experimental section

All reagents and solvents were employed as received. Bismuth(III) nitrate pentahydrate (≥98.0%), zirconyl chloride octahydrate (98.0%), vanadium(IV)-oxy acetylacetonate (98.0%), sodium hydroxide (pellets for analysis), tetrabutylammonium perchlorate (≥99.0% electrochemical degree), benzyl alcohol (anhydrous 99.8%), ferrocene (98.0%), anisole (≥99.0%), *tert*-butyl alcohol (≥99.0%), 1,4-diazabicyclo{2.2.2}octane (DABCO, ≥99.0%) and dimethylsulfoxide (anhydrous) were purchase from Sigma Aldrich; ethyleneglycol (technical degree) and acetonitrile (HPLC) were purchase from Scharlab; deuterated acetonitrile (99.8% D) was purchased from Eurisotop. Anhydrous acetonitrile (HPLC, SPS M BRAUN) was obtained from an SPS M Braun System.

Preparation and characterization of Zr decorated $BiVO_4$ photoanodes

The synthesis and fabrication of 2.5% zirconium $BiVO_4$ electrodes was performed following the literature procedure.[31] This procedure consists of electrodeposition of a $Bi(NO_3)_3 \cdot 5H_2O$ (20 mM) and $ZrCl_2O \cdot 8H_2O$ (0.5 mM) solution in ethyleneglycol followed by drop-coating of a solution of $VO(acac)_2$ (0.15 M) in DMSO. Absorbance spectra of the $BiVO_4$ photoanodes were measured on a Varian Cary 300 Bio spectrophotometer. Powder X-ray diffraction data were acquired on a Rigaku Miniflex 600 (Rigaku Corporation, Tokyo, Japan) with copper Kα radiation (λ = 1.5418 Å) at a scan speed of 3° min^{-1}. Finally, scanning electron microscopy (SEM) images were recorded with a Leica-Zeiss LEO 440 microscopy. To improve the quality of the images, the top of the samples was covered with platinum. The UV-vis spectra, X-ray diffraction (XRD) data and surface morphology were consistent with the ones described in the literature (see Fig. S1†).

(Photo)electrochemical measurements

Photoelectrochemical and electrochemical measurements were performed on a PGSTAT302N potentiostat (Metrohm-Autolab, The Netherlands) in a one-compartment, three-electrode configuration photoelectrochemical solar cell (PEC). Non-aqueous $Ag/AgNO_3$ (ALS, Japan) and platinum foil (0.1 mm thick, Alfa Aesar) constitute the reference and counter electrodes and a solution of 0.1 M of tetrabutylammonium perchlorate ($TBAClO_4$) in CH_3CN was the non-aqueous electrolyte selected as the supporting electrolyte. PECs were illuminated using an ozone-free 300 W xenon (Xe) lamp and the illumination of the working photoelectrode was adjusted with a thermopile to 100 mW cm^{-2}. CV measurements were carried out at 50 mV s^{-1} and all the electrochemical measurements were referred to the reference electrode $Ag/AgNO_3$. Experiments were performed at V_{oc}, 0.4, 0.8, 1.2 and 1.6 V *vs.* $Ag/AgNO_3$, V_{oc} being the potential reached when illuminating the sample under open circuit conditions, *i.e.* without applying a potential (typically −0.2 V *vs.* $Ag/AgNO_3$).

To refer the photoelectrochemical potentials to the reversible hydrogen electrode (RHE), the ferrocene/ferrocenium (Fc/Fc^+) couple was used as an internal reference by adding 2.0 mM ferrocene after the electrochemical tests (see Fig. S2†).

In typical chronoamperometry (CA), the corresponding concentration of benzyl alcohol (**1**) was added to a solution of 30 mL of electrolyte. Half of the solution was kept in a vial and labelled the blank sample. The other half was introduced in a transparent quartz PEC, with dimensions of 5 × 3 × 5 cm^3, and was used for chronoamperometry. Before the CA measurement, CV in the dark and under light was used to test the performance of the electrode. CA measurements were run under soft stirring and constant potential for 13 hours. The CA measurements were performed for 5 s each and the faradaic yield was estimated by integration of the current, adapting the Faraday law of electrolysis to our case (eqn (1)).

$$F_{\text{yield}} = \frac{n_{\mathbf{2}}}{n_{\mathbf{1},0}} \times 100 = \frac{Q}{n_e F n_{\mathbf{1},0}} \times 100 = \frac{\int I\,dt}{n_e F n_{\mathbf{1},0}} \times 100 \approx \frac{\sum I \Delta t}{2 F n_{\mathbf{1},0}} \times 100 \quad (1)$$

where $n_{\mathbf{1},o}$ is the initial number of moles of **1**, $n_{\mathbf{2}}$ is the number of moles of benzaldehyde produced (**2**), n_e is the number of electrons needed in the reaction (n_e = 2 in this case), F is the Faraday constant, I is the current and Δt is the time step.

As a Xe lamp has visible and UV light, bandpass filters were used to select the wavelength of incident light when needed. Experiments with visible light were carried out using a long wavelength pass UV filter (S&K); experiments with UV light were carried out using two coupled short wavelength pass filters of 400 nm and 475 nm (Edmund Optics). Filters were placed in the middle between the lamp and PEC. Considering the part of the light absorbed by the filters, the final illumination power in the photoelectrode was 100 mW cm^{-2}, measured with a thermopile, unless explicitly indicated.

Electrode-free reactions with light

Studies under an inert atmosphere were performed using anhydrous CH_3CN (N_2 atmosphere), in a Schlenk flask with 100 mM **1**, illuminated with an ozone-free Xe lamp (100 mW cm^{-2}). The reaction under O_2 was performed similarly but by saturating the solution with O_2.

Photocatalytic endoperoxidation of anthracene

A solution of anthracene (0.5 mg mL^{-1}) in CD_3CN was illuminated with an ozone-free Xe lamp (100 mW cm^{-2}) in the absence and presence of O_2. Reactions were monitored by ^1H NMR. When needed, DABCO (0.5 mg mL^{-1}) was used as an $^1O_2$ quencher.

Analytical measurements

The analytical performance of the reactions was measured by ^{1}H NMR spectroscopy. NMR spectra were recorded, under ambient temperature, on a Bruker 400/300 MHz instrument. For this purpose, CD_3CN and anisole were used as the solvent and integration reference standard.

Results and discussion

With the aim of investigating the photoelectrochemical oxidation of primary alcohols, we used a Zr-decorated $BiVO_4$ photoanode, due to its proven oxidation capabilities.[31] In order to avoid competition with water oxidation, and aiming to ensure solubility of reagents and products while maximizing the stability of our $BiVO_4$ electrodes, we used acetonitrile as the solvent.[9] We studied the photoelectrooxidation of benzyl alcohol (**1**) to benzaldehyde (**2**) (Scheme 1), which constitutes a convenient model reaction for study because the reaction can be easily monitored by ^{1}H NMR spectroscopy and gas chromatography (GC).

The electrooxidation of **1** (2 mM in CH_3CN) was performed using a Pt microelectrode for oxidation as the working electrode (WE), Pt film as the counter electrode (CE), and 0.1 M tetrabutylammonium perchlorate ($TBAClO_4$) as the electrolyte. All measurements were referenced against $Ag/AgNO_3$. The cyclic voltammetry curve shown in Fig. 1a shows an oxidation wave at 1.94 V, which is attributed to the oxidation of **1** to **2**.[32] When the working electrode is replaced by $BiVO_4$, in the absence of **1** under dark conditions, no current was detected below 2 V. However, a photocurrent was observed upon illumination (ozone-free Xe lamp 100 mW cm^{-2}) (Fig. 1b). This photocurrent observed in the absence of **1** can be attributed to the presence of traces of water in the system (see Fig. S3†). In the presence of **1** and in the dark, almost negligible differences in the oxidation potential for both electrodes (Pt and $BiVO_4$, see Fig. S4†) are observed. However, under illumination, a significant shift to lower potentials (+0.45 V) was observed when using $BiVO_4$, due to the photoelectroactivity of the electrode. This potential is similar to the ones reported previously when $BiVO_4/WO_3$ photoanodes were used for the oxidation of benzylic alcohols.[10]

We next performed a series of chronoamperometry experiments with light for the oxidation of **1** (100 mM) at different voltages (open circuit voltage V_{oc}, 0.4, 0.8, 1.2 and 1.6 V *vs.* $Ag/AgNO_3$) during 13 h, illuminated with an ozone-free Xe lamp at 100 mW cm^{-2}. At the end of each experiment, the product yield was determined by ^{1}H NMR spectroscopy. As can be observed in Fig. 2a, together with the formation of benzaldehyde (**2**), a significative amount of benzoic acid (**3**) was also detected at each potential. The production of **3** is a consequence of the overoxidation of **1**. The combined yield of both, **2** and **3**, increased with the potential, with no significant changes upon potentials above 1.2 V. Surprisingly, at V_{oc}, non-negligible yields of 25 and 5% were obtained for **2** and **3**, respectively. Moreover, chronoamperometry at V_{oc} led to the formation of H_2O_2 in a 1 : 1 molar ratio with respect to **2**. Identification and quantification of H_2O_2 were performed by ^{1}H NMR, by comparing with the ^{1}H NMR spectrum of H_2O_2 in the same deuterated solvent and integrating against anisole as the integration reference standard (see ESI Fig. S5† for further details). It is worth mentioning that the detection of H_2O_2 in the photoelectrochemical oxidation of alcohols has previously been reported, although its origin remains unclear.[33]

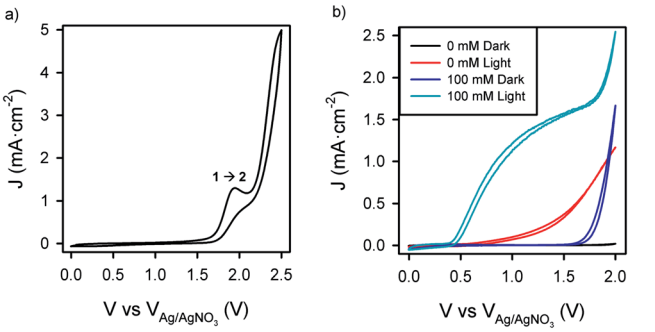

Fig. 1 Cyclic voltammetry of benzyl alcohol (**1**). (a) 2 mM **1** in 0.1 M $TBAClO_4$ in CH_3CN, using a Pt microelectrode as the WE, Pt film as the counter electrode (CE) and $Ag/AgNO_3$ as the reference electrode (RE). Oxidation peak of **1** to benzaldehyde (**2**) is observed (**1** → **2**). (b) 0 and 100 mM **1** (benzyl alcohol), in 0.1 M $TBAClO_4$ in CH_3CN, using Zr decorated $BiVO_4$ as the WE, a Pt film as the CE and $Ag/AgNO_3$ as the RE. The cyclic voltammetry in this case was performed under dark and light conditions. Illumination was performed with an ozone-free Xe lamp 100 mW cm^{-2}.

The Faraday yield (obtained from the Faraday law, eqn (1)) was also determined at each potential, being negligible at V_{oc} (as expected) and showing no significant changes above 1.2 V (Fig. 2b). Interestingly, we also observed that, at all potentials, the amount of product determined by NMR was larger than the expected amount according to the Faraday yield. In addition, the difference between these two yields (NMR and Faraday) remained virtually constant for each potential. This result strongly suggests that a parallel pathway, different from the photoelectrochemical oxidation of **1**, occurs during the chronoamperometric oxidation of **1**.

We thought that this non-electrochemical oxidation could be due to the following reasons: (i) thermal effect, (ii) photocatalytic activity of $BiVO_4$, (iii) activation by $^{\bullet}OH$ radicals,[8] (iv) light-driven photooxidation, or (v) autocatalytic oxidation of benzyl alcohol, as suggested in previous studies.[30] Considering that in the chronoamperometry, after illuminating for 13 hours, the solutions reach a temperature of 313 K, we performed the reaction at this temperature, without applying bias or illumination. Under these conditions, no reaction was detected (Table

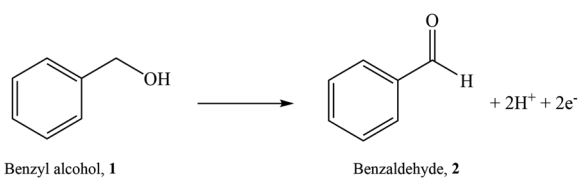

Scheme 1 Oxidation of benzyl alcohol (**1**) to benzaldehyde (**2**).

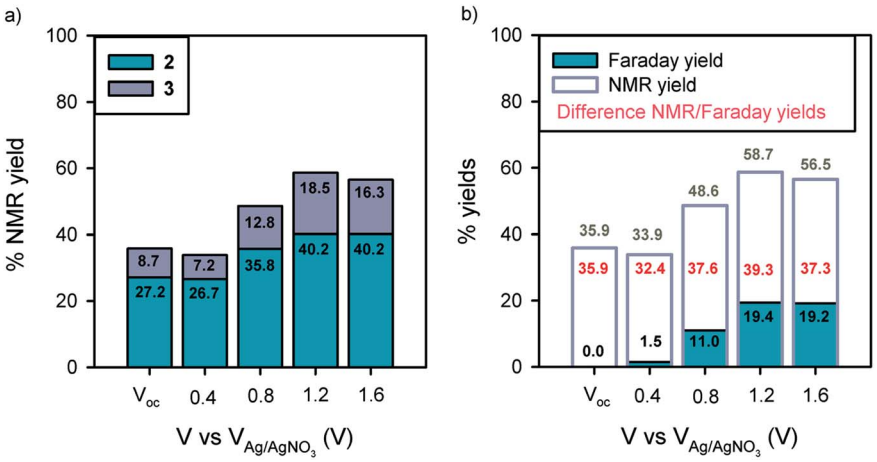

Fig. 2 Chronoamperometry experiments for the oxidation of benzyl alcohol (**1**) at different potentials, under illumination with an ozone-free Xe lamp at 100 mW cm^{-2}. Conditions: 100 mM **1**, in 0.1 M TBAClO$_4$ in CH$_3$CN, using Zr decorated BiVO$_4$ as the WE, a Pt film as the CE and Ag/AgNO$_3$ as the RE. (a) Yield of oxidation of **1** to benzaldehyde (**2**) and benzoic acid (**3**) calculated by ^{1}H NMR, using 100 mM anisole as the integration reference standard. (b) Comparison between total product yield (yield of **2** + yield of **3**) obtained by ^{1}H NMR and Faraday yield. Details for calculation of the Faraday yield are in the Experimental section.

Table 1 Reactions under different conditions[a]

Entry	Light conditions	BiVO$_4$	Applied bias (V)	Atmosphere	Yield[b] (%) **2**	**3**
1[c]	UV-vis	Yes	1.6	O$_2$	40.2	16.3
2[d]	Dark	Yes	V_{oc}	O$_2$	0.0	0.0
3	Vis	Yes	V_{oc}	O$_2$	0.0	0.0
4[e]	UV-vis	Yes	1.6	O$_2$	40	16
5	UV-vis	No	—	O$_2$	22.7	2.2
6	UV	No	—	O$_2$	27.8	3.3
7	Vis	No	—	O$_2$	0.0	0.0
8	UV	No	—	N$_2$	0.0	0.0

[a] Reaction conditions: 100 mM **1** in 15 mL of CH$_3$CN during 13 hours, illumination with an ozone-free Xe lamp at 100 mW cm^{-2}, with filters used when needed. [b] ^{1}H NMR using 100 mM anisole as the integration reference standard. [c] Data from Fig. 2a. [d] Temperature of 313 K. [e] Using 5 mM *tert*-butyl alcohol as the $^{\bullet}$OH scavenger.

1, entry 2); therefore, the overoxidation due to a thermal process can be discarded.

When the reaction was carried out with BiVO$_4$ at V_{oc}, without applying bias, illuminating with visible light, no oxidation of **1** was detected. This experiment made us discard the hypothesis that the photocatalytic activity of BiVO$_4$ was responsible for the overoxidation of the alcohol (Table 1, entry 3).

Ye and co-workers recently pointed out that benzyl alcohol can be oxidized through a radical relay strategy coupled to water oxidation.[8] In this process, $^{\bullet}$OH radicals are formed and are responsible for the oxidation of the alcohol. Considering that we have traces of water in our system (Fig. 1b and S3†), we decided to check whether $^{\bullet}$OH radicals could be responsible for the oxidation of **1**. For this purpose, we performed the chronoamperometry experiment in the presence of *tert*-butyl alcohol, a $^{\bullet}$OH scavenger. Under these conditions, we did not observe any modification in the amount of **2** formed; thus the participation of $^{\bullet}$OH radicals can be discarded in our case (Table 1, compare entries 1 and 4).

In the absence of BiVO$_4$, after illuminating with UV light for 13 hours in the presence of air, **2** and **3** were obtained (see Table 1, entries 5 and 6), with the concomitant production of H_2O_2. The differences found between the yields in entries 5 and 6 are due to a larger UV power used in the case of illuminating only with UV light. Moreover, in the absence of BiVO$_4$, but illuminating with visible light or under inert atmosphere, no reaction was observed (Table 1, entries 7 and 8). These observations indicate that the non-electrochemical oxidation reaction is observed only for samples irradiated with UV-light under air.

Photocatalyzed processes involving reactive oxygen species (ROS), such as $^1O_2$, constitute an effective method for the oxidation of many organic species, as well as for synthesizing oxygenated molecules by facilitating carbon–oxygen and heteroatom–oxygen bond formation.[34–37] Considering that from our results in Table 1 we can conclude that the combination of UV light and O_2 leads to a non-electrochemical path for the oxidation of **1**, we decided to explore whether singlet oxygen ($^1O_2$, $^1\Delta_g$) could be formed under our reaction conditions and provoke the non-electrochemical oxidation of **1**. Anthracenes have widely been used for the detection and quantification of singlet oxygen production.[38–42] In order to determine if $^1O_2$ is formed when illuminating with UV light, we illuminated an oxygenated solution of anthracene (3 mM) in CD$_3$CN with a Xe lamp, and we monitored the reaction by ^{1}H NMR spectroscopy. After 10 minutes, anthracene was converted into 9,10-dihydro-9,10-epidioxyanthracene (anthracene-endoperoxide) in 58% yield (Fig. 3a and b). Under the same reaction conditions, but using an oxygen-free solution, anthracene-endoperoxide was not detected. In addition, when the reaction was performed in the presence of a singlet oxygen quencher, such as 1,4-diazabicyclo{2.2.2}octane (DABCO), under aerobic conditions and under UV irradiation, again anthracene-endoperoxide was not

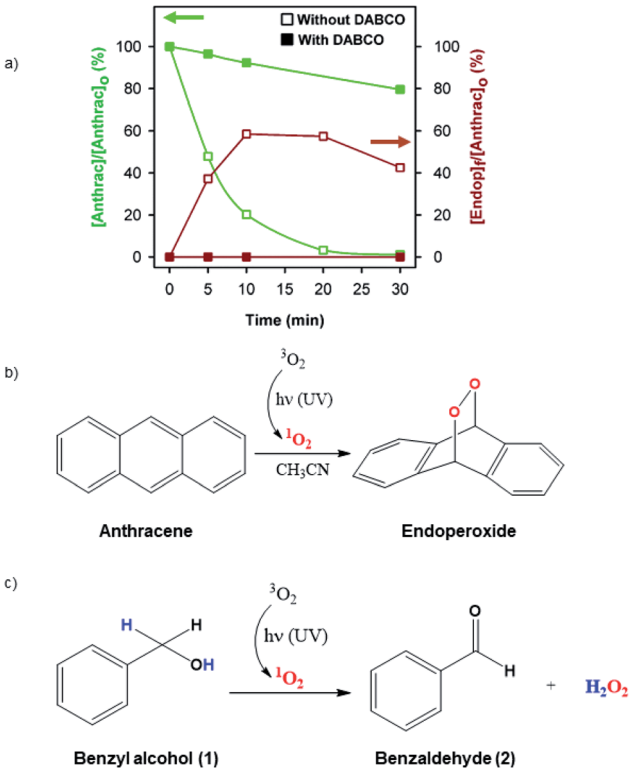

Fig. 3 (a) Time evolution of the conversion of anthracene (left axis) and formation of endoperoxide, during the illumination of a solution of anthracene (0.5 mg mL^{-1}) in CD_3CN, in the absence or presence of DABCO (1 : 1 molar ratio with anthracene). Illumination was performed with an ozone-free Xe lamp at 100 mW cm^{-2}. ^1H % conversion of anthracene and % formation of endoperoxide were calculated by ^1H NMR. After 20 min of illumination without DABCO, degradation of endoperoxide was detected, explaining the decrease in the concentration of endoperoxide at 30 min. (b) Scheme of endoperoxide formation by the reaction of anthracene and $^1O_2$. (c) Proposed reaction scheme for the oxidation of benzyl alcohol (**1**) with $^1O_2$, leading to the formation of H_2O_2.

formed (Fig. 3a).[43] Interestingly, when a solution of **1** was irradiated with UV light in the presence of DABCO no conversion of **1** into **2** was observed (Table S1,† entry 5). All these experiments clearly demonstrate that $^1O_2$ is formed when illuminating with UV light. This formation of $^1O_2$ explains the non-electrochemical oxidation of **1**, depicted in Fig. 3c; therefore we can exclude the hypothesis that other pathways, such as the autocatalytic oxidation of **1** reported previously,[30] is taking place in our case. The reaction depicted in Fig. 3c also explains the formation of H_2O_2 that we detect in our process.

Once we confirmed the generation of $^1O_2$ under UV light irradiation, we carried out a series of chronoamperometry experiments by illuminating with visible light (Table 2) in order to eliminate the contribution of the non-electrochemical reaction. At V_{oc} no conversion of **1** was observed (Table 2, entry 1), confirming that no photocatalytic conversion at the surface of $BiVO_4$ occurs in this system. When applying external bias, **1** was selectively oxidized to **2**, without formation of the over-oxidized species **3** or H_2O_2. This result corroborates that the over-oxidation of the aldehyde and formation of H_2O_2 are both

Table 2 Chronoamperometry experiments under visible light at different voltages[a]

Entry	V (V) *vs.* $V_{Ag/AgNO_3}$	NMR yield[b]	Faradaic efficiency[c] (%)	H_2O_2
1	V_{oc}	0.0	—	No
2	0.4	2.8	100	No
3	0.8	10.2	100	No
4	1.2	13.1	100	No
5	1.6	13.4	100	No

[a] Reaction conditions: 100 mM benzyl alcohol in 0.1 M $TBAClO_4$ in CH_3CN solution, using Zr decorated $BiVO_4$ as the WE, a Pt film as the CE and $Ag/AgNO_3$ as the RE. Illumination with an ozone-free Xe lamp at 100 mW cm^{-2} using a long wavelength pass UV filter, to ensure only illumination with visible light. Irradiance over the sample was 85 mW cm^{-2}. [b] ^1H NMR yield of benzaldehyde (2) using 100 mM anisole as the integration reference standard. [c] Faradaic efficiency calculated as 'NMR yield/Faraday yield'.

exclusively due to a UV-induced generation of $^1O_2$. Furthermore, we observed that under visible light, the oxidation of benzyl alcohol takes place exclusively through the photo-electrochemical conversion path, as the Faraday yield matched perfectly with the NMR yield.

As can be seen in Table 2, an enhancement in the yield of **2** was observed at higher voltages. This result agrees with the increase of photocurrent observed by cyclic voltammetry under visible light (see Fig. S6 in the ESI†), which by other side, has the same shape as the cyclic voltammetry under UV-vis illumination (Fig. 1b). Under these conditions, the Faraday yield matched perfectly with the NMR yield. In addition, no H_2O_2 was detected at V_{oc} (or any other applied voltage), demonstrating that H_2O_2 is exclusively produced by the UV-induced generation of $^1O_2$.

The data shown in Tables 1 and 2 allowed us to quantify the contribution of the formation of **2** due to UV light/singlet oxygen in the process. Thus, of the 40% yield achieved for the oxidation of **1** to **2** (Table 1, entries 1 and 4), 22.7% can be directly attributed to the oxidation produced by singlet oxygen under UV irradiation that occurs in the absence of the photoanode (Table 1, entry 5), and 13.4% of the yield is due to the activity of the $BiVO_4$ under illumination with visible (not UV) light (Table 2, entry 5). This leaves just 3.9% yield that can be assigned to the contribution of the activity of the photoanode. By other side, the number of UV photons emitted by the Xe lamp is smaller than the amount of photons present in the visible region of its spectrum. As the absorbance of $BiVO_4$ is nearly constant from 200 to 550 nm,[44] the number of absorbed photons effectively transformed into electrons is still larger in the visible than in the UV region of the spectra.

Conclusions

In conclusion, the photoelectrochemical oxidation of benzyl alcohol to benzaldehyde using $BiVO_4$ anodes was studied, and the factors affecting this transformation were analysed. A non-electrochemical path for the oxidation of the alcohol has been found for the first time. We demonstrated that this alternative oxidation process is due to the formation of singlet oxygen in

the reaction media, as a consequence of the use of UV light and the presence of oxygen. The formation of $^1O_2$ explains the formation of hydrogen peroxide, which leads to the over-oxidation of the alcohol. In fact, we observed that $^1O_2$-mediated production of **2** is dominant over the photoelectrocatalytic process, while the contribution of the direct photocatalytic reaction is almost negligible. This additional oxidation path justifies the strong activation of the reaction under UV light that remarkably enhances the amount of aldehyde obtained with respect to the photoelectrochemical oxidation. Our findings demonstrate that any studies using photoelectrocatalytic oxidation under UV light irradiation should seriously consider the results published herein, in order to avoid the misinterpretations of the photoanode's efficiency, which can lead to the overestimation of the activity.

Conflicts of interest

The authors declare no competing financial interest.

Acknowledgements

The authors would like to acknowledge the Ministerio de Economía y Competitividad (MINECO) of Spain (ENE2017-85087-C3-1-R and PGC2018-093382-B-I00) and University Jaume I (UJI-B2019-20 and UJI-B2017-07). Serveis Centrals d'Instrumentació Científica at UJI is acknowledged for NMR measurements.

Notes and references

1 Y. Tachibana, L. Vayssieres and J. R. Durrant, Artificial photosynthesis for solar water-splitting, *Nat. Photonics*, 2012, **6**(8), 511–518.
2 M. Grätzel, Photoelectrochemical cells, *Nature*, 2001, **414**(6861), 338–344.
3 A. Fujishima and K. Honda, Electrochemical Photolysis of Water at a Semiconductor Electrode, *Nature*, 1972, **238**(5358), 37–38.
4 S. Jin, What Else Can Photoelectrochemical Solar Energy Conversion Do Besides Water Splitting and CO_2 Reduction?, *ACS Energy Lett.*, 2018, **3**(10), 2610–2612.
5 K. Sayama, Production of High-Value-Added Chemicals on Oxide Semiconductor Photoanodes under Visible Light for Solar Chemical-Conversion Processes, *ACS Energy Lett.*, 2018, **3**(5), 1093–1101.
6 S. D. Tilley, Recent Advances and Emerging Trends in Photo-Electrochemical Solar Energy Conversion, *Adv. Energy Mater.*, 2019, **9**(2), 1802877.
7 H. G. Cha and K. S. Choi, Combined biomass valorization and hydrogen production in a photoelectrochemical cell, *Nat. Chem.*, 2015, **7**(4), 328–333.
8 L. Luo, Z.-j. Wang, X. Xiang, D. Yan and J. Ye, Selective Activation of Benzyl Alcohol Coupled with Photoelectrochemical Water Oxidation via a Radical Relay Strategy, *ACS Catal.*, 2020, **10**(9), 4906–4913.
9 T. Li, T. Kasahara, J. He, K. E. Dettelbach, G. M. Sammis and C. P. Berlinguette, Photoelectrochemical oxidation of organic substrates in organic media, *Nat. Commun.*, 2017, **8**(1), 390.
10 H. Tateno, Y. Miseki and K. Sayama, Photoelectrochemical Oxidation of Benzylic Alcohol Derivatives on $BiVO_4/WO_3$ under Visible Light Irradiation, *ChemElectroChem*, 2017, **4**(12), 3283–3287.
11 W. Fang, R. Tao, Z. Jin, Z. Sun, F. Li and L. Xu, Sandwich-type cobalt-polyoxometalate as an effective hole extraction layer for enhancing $BiVO_4$-based photoelectrochemical oxidation, *J. Alloys Compd.*, 2019, **797**, 140–147.
12 H. Tateno, Y. Miseki and K. Sayama, Photoelectrochemical dimethoxylation of furan via a bromide redox mediator using a $BiVO_4/WO_3$ photoanode, *Chem. Commun.*, 2017, **53**(31), 4378–4381.
13 H. Tateno, S. Iguchi, Y. Miseki and K. Sayama, Photo-Electrochemical C–H Bond Activation of Cyclohexane Using a WO_3 Photoanode and Visible Light, *Angew. Chem., Int. Ed.*, 2018, **57**(35), 11238–11241.
14 H. Tateno, Y. Miseki and K. Sayama, PINO/NHPI-mediated selective oxidation of cycloalkenes to cycloalkenones via a photo-electrochemical method, *Chem. Commun.*, 2019, **55**(63), 9339–9342.
15 L.-W. Huang, T.-G. Vo and C.-Y. Chiang, Converting glycerol aqueous solution to hydrogen energy and dihydroxyacetone by the $BiVO_4$ photoelectrochemical cell, *Electrochim. Acta*, 2019, **322**, 134725.
16 J. Liu, J. Li, M. Shao and M. Wei, Directed synthesis of SnO_2@$BiVO_4$/Co–Pi photoanode for highly efficient photoelectrochemical water splitting and urea oxidation, *J. Mater. Chem. A*, 2019, **7**(11), 6327–6336.
17 H. He, J. Du, B. Wu, X. Duan, Y. Zhou, G. Ke, T. Huo, Q. Ren, L. Bian and F. Dong, Photoelectrochemical driving and clean synthesis of energetic salts of 5,5′-azotetrazolate at room temperature, *Green Chem.*, 2018, **20**(16), 3722–3726.
18 L. Zhang, L. Liardet, J. Luo, D. Ren, M. Grätzel and X. Hu, Photoelectrocatalytic arene C–H amination, *Nat. Catal.*, 2019, **2**(4), 366–373.
19 T. Mallat and A. Baiker, Oxidation of Alcohols with Molecular Oxygen on Solid Catalysts, *Chem. Rev.*, 2004, **104**(6), 3037–3058.
20 F. Su, S. C. Mathew, G. Lipner, X. Fu, M. Antonietti, S. Blechert and X. Wang, mpg-C_3N_4-Catalyzed Selective Oxidation of Alcohols Using O_2 and Visible Light, *J. Am. Chem. Soc.*, 2010, **132**(46), 16299–16301.
21 C. Parmeggiani and F. Cardona, Transition metal based catalysts in the aerobic oxidation of alcohols, *Green Chem.*, 2012, **14**(3), 547–564.
22 Z. Shi, C. Zhang, C. Tang and N. Jiao, Recent advances in transition-metal catalyzed reactions using molecular oxygen as the oxidant, *Chem. Soc. Rev.*, 2012, **41**(8), 3381–3430.
23 S. E. Davis, M. S. Ide and R. J. Davis, Selective oxidation of alcohols and aldehydes over supported metal nanoparticles, *Green Chem.*, 2013, **15**(1), 17–45.

24 S. Wertz and A. Studer, Nitroxide-catalyzed transition-metal-free aerobic oxidation processes, *Green Chem.*, 2013, **15**(11), 3116–3134.
25 Z. Guo, B. Liu, Q. Zhang, W. Deng, Y. Wang and Y. Yang, Recent advances in heterogeneous selective oxidation catalysis for sustainable chemistry, *Chem. Soc. Rev.*, 2014, **43**(10), 3480–3524.
26 J. C. Colmenares, W. Ouyang, M. Ojeda, E. Kuna, O. Chernyayeva, D. Lisovytskiy, S. De, R. Luque and A. M. Balu, Mild ultrasound-assisted synthesis of TiO_2 supported on magnetic nanocomposites for selective photo-oxidation of benzyl alcohol, *Appl. Catal., B*, 2016, **183**, 107–112.
27 S. Kim and W. Choi, Visible-Light-Induced Photocatalytic Degradation of 4-Chlorophenol and Phenolic Compounds in Aqueous Suspension of Pure Titania: Demonstrating the Existence of a Surface-Complex-Mediated Path, *J. Phys. Chem. B*, 2005, **109**(11), 5143–5149.
28 G. Palmisano, G. Scandura, V. Augugliaro, V. Loddo, A. Pace, B. S. Tek, S. Yurdakal and L. Palmisano, Unexpectedly ambivalent O_2 role in the autocatalytic photooxidation of 2-methoxybenzyl alcohol in water, *J. Mol. Catal. A: Chem.*, 2015, **403**, 37–42.
29 H. Li, F. Qin, Z. Yang, X. Cui, J. Wang and L. Zhang, New Reaction Pathway Induced by Plasmon for Selective Benzyl Alcohol Oxidation on BiOCl Possessing Oxygen Vacancies, *J. Am. Chem. Soc.*, 2017, **139**(9), 3513–3521.
30 M. J. Pavan, H. Fridman, G. Segalovich, A. I. Shames, N. G. Lemcoff and T. Mokari, Photooxidation of Benzyl Alcohol with Heterogeneous Photocatalysts in the UV Range: The Complex Interplay with the Autoxidative Reaction, *ChemCatChem*, 2018, **10**(12), 2541–2545.
31 M. N. Shaddad, M. A. Ghanem, A. M. Al-Mayouf, S. Gimenez, J. Bisquert and I. Herraiz-Cardona, Cooperative Catalytic Effect of ZrO_2 and α-Fe_2O_3 Nanoparticles on $BiVO_4$ Photoanodes for Enhanced Photoelectrochemical Water Splitting, *ChemSusChem*, 2016, **9**(19), 2779–2783.
32 H. Lund, Electroorganic Preparations. II. Oxidation of Carbinols, *Acta Chem. Scand.*, 1957, **11**, 491–498.
33 D. Liu, J.-C. Liu, W. Cai, J. Ma, H. B. Yang, H. Xiao, J. Li, Y. Xiong, Y. Huang and B. Liu, Selective photoelectrochemical oxidation of glycerol to high value-added dihydroxyacetone, *Nat. Commun.*, 2019, **10**(1), 1779.
34 A. A. Ghogare and A. Greer, Using Singlet Oxygen to Synthesize Natural Products and Drugs, *Chem. Rev.*, 2016, **116**(17), 9994–10034.
35 Y. Nosaka and A. Y. Nosaka, Generation and Detection of Reactive Oxygen Species in Photocatalysis, *Chem. Rev.*, 2017, **117**(17), 11302–11336.
36 A. Greer, Christopher Foote's Discovery of the Role of Singlet Oxygen [$^1O_2$ ($^1\Delta_g$)] in Photosensitized Oxidation Reactions, *Acc. Chem. Res.*, 2006, **39**(11), 797–804.
37 V. Martínez-Agramunt and E. Peris, Photocatalytic Properties of a Palladium Metallosquare with Encapsulated Fullerenes via Singlet Oxygen Generation, *Inorg. Chem.*, 2019, **58**(17), 11836–11842.
38 R. Vankayala, A. Sagadevan, P. Vijayaraghavan, C.-L. Kuo and K. C. Hwang, Metal Nanoparticles Sensitize the Formation of Singlet Oxygen, *Angew. Chem., Int. Ed.*, 2011, **50**, 10640–10644.
39 S. Xu, P. Zhou, Z. Zhang, C. Yang, B. Zhang, K. Deng, S. Bottle and H. Zhu, Selective Oxidation of 5-Hydroxymethylfurfural to 2,5-Furandicarboxylic Acid Using O_2 and a Photocatalyst of Co-thioporphyrazine Bonded to g-C_3N_4, *J. Am. Chem. Soc.*, 2017, **139**(41), 14775–14782.
40 A. Sagadevan, K. C. Hwang and M.-D. Su, Singlet oxygen-mediated selective C–H bond hydroperoxidation of ethereal hydrocarbons, *Nat. Commun.*, 2017, **8**(1), 1812.
41 J. M. de Souza, T. J. Brocksom, D. T. McQuade and K. T. de Oliveira, Continuous Endoperoxidation of Conjugated Dienes and Subsequent Rearrangements Leading to C–H Oxidized Synthons, *J. Org. Chem.*, 2018, **83**(15), 7574–7585.
42 Y. You, Chemical tools for the generation and detection of singlet oxygen, *Org. Biomol. Chem.*, 2018, **16**(22), 4044–4060.
43 W.-J. Kwak, S. A. Freunberger, H. Kim, J. Park, T. T. Nguyen, H.-G. Jung, H. R. Byon and Y.-K. Sun, Mutual Conservation of Redox Mediator and Singlet Oxygen Quencher in Lithium–Oxygen Batteries, *ACS Catal.*, 2019, **9**(11), 9914–9922.
44 J. Han, K. Li, H. Cheng and L. Zhang, A Green Desulfurization Technique: Utilization of Flue Gas SO_2 to Produce H_2 via a Photoelectrochemical Process Based on Mo-Doped $BiVO_4$, *Front. Chem.*, 2017, **5**, 114.

